


 Cite this: *RSC Adv.*, 2022, 12, 30167

Synthesis and properties of high performance thermoplastic polycarbonate polyurethane elastomers through a non-isocyanate route†

 Tong Liu,^{ab} Xiangui Yang,^{id} *^a Shuqing Zhang,^a Qingyin Wang,^a Ning Jiang^c and Gongying Wang^a

Thermoplastic polycarbonate polyurethane elastomers (TPCUEs) are synthesized through a solvent-free non-isocyanate melt polycondensation route. The route starts with the synthesis of 1,6-bis(hydroxyethyloxycarbonylamino)hexane (BHCH) from ethylene carbonate and 1,6-hexanediamine, and then the TPCUEs are prepared by the melt polycondensation of BHCH and polycarbonate diols (PCDLs). The TPCUEs are characterized by GPC, FT-IR, ¹H NMR, XRD, AFM, DSC, TGA and tensile testing. The TPCUEs prepared have linear structures and high molecular weights, with M_n over 3.0×10^4 g mol⁻¹. And these TPCUEs exhibit excellent thermal and mechanical properties, with T_g ranging from -18 to -1 °C, T_m ranging from 93 to 122 °C, $T_{d,5\%}$ over 240 °C, tensile strength between 28.1–47.3 Mpa, elongation at break above 1000%, Young's modulus between 13.8–32.7 Mpa and resilience at 200% fixed-length between 70–90%, which makes them a promising alternative to products synthesized through the isocyanate route. In addition, the effects of the hard segment contents and the molecular weights of soft segment on the properties of TPCUEs are researched.

 Received 6th September 2022
 Accepted 12th October 2022

DOI: 10.1039/d2ra05613e

rsc.li/rsc-advances

Introduction

Polyurethanes (PUs) are an important class of polymers that are widely used as elastomers, foams, coatings, adhesives and medical materials due to their extraordinary physical and chemical properties, such as toughness, biocompatibility, wear resistance and elasticity.^{1,2} Thermoplastic polyurethane elastomers (TPUEs) play an irreplaceable role in a wide range of applications with their excellent mechanical and processing properties.³ Traditionally, TPUEs are synthesized in a stepwise polymerization process of oligomeric diols and diisocyanates with chain extenders, with the isocyanates and chain extenders forming the hard chain segments and the oligodiols forming the soft chain segments.⁴ Oligomeric ether diols, oligomeric diols and oligomeric carbonate diols are commonly used as oligomeric alcohol reactants.^{5,6}

The main problems associated with the synthesis of TPUEs by conventional methods are the toxicity of diisocyanates and their sensitivity to moisture. Isocyanates are highly toxic

chemicals that can cause irreversible damage to the eyes and respiratory system.^{7,8} Moreover, isocyanates are usually obtained industrially through the more toxic phosgene. In addition, during the synthesis process, isocyanates readily react with water of raw materials or in the air to generate carbon dioxide gas, which causes bubbles to form in the materials, and while it is needed in foam synthesis, it is undesirable in the synthesis of TPUEs.⁹ Therefore, non-isocyanate routes that do not use isocyanates have attracted great interest from researchers in recent years.^{10–12}

The non-isocyanate routes allow the synthesis of TPUEs by stepwise polymerization or condensation polymerization.^{12,13} Stepwise polymerization of diamines and dicyclic carbonates has been extensively studied, and TPUEs prepared in this way are called polyhydroxycarbamates due to the hydroxyl groups on their repeating units.^{1,10,14–16} The presence of hydroxyl groups in the side chains leads to the formation of inter and intra molecular hydrogen bonds with the carbamate carbonyl groups, and as a result, some properties of polyhydroxycarbamates like resistance to permeation and adhesion perform better than typical PUs.¹⁷ However, this route requires solvents and relatively long reaction time, and the preparation of the required dicyclic carbonates is complicated, especially for large molecules with complex structures.

TPUEs synthesized by condensation polymerization have similar structures and properties as classical PUs, and the reactions are mostly solvent-free and environmentally friendly. Bisalkyl carbamates and bishydroxyalkyl carbamates are

^aChengdu Institute of Organic Chemistry, Chinese Academy of Sciences, Chengdu 610041, Sichuan, China. E-mail: yangxg@cioc.ac.cn

^bNational Engineering Laboratory for VOCs Pollution Control Material & Technology, University of Chinese Academy of Sciences, Beijing 100049, China

^cSchool of Chemical Engineering, Sichuan University of Science & Engineering, Zigong, 643000, Sichuan, China

† Electronic supplementary information (ESI) available. See DOI: <https://doi.org/10.1039/d2ra05613e>



commonly used as raw materials for the synthesis of TPUEs by condensation polymerization. Bisalkyl carbamates can be synthesized from dimethyl carbonate (DMC) with diamines, several reports have investigated this method in recent years.^{18–23} Shen *et al.* found experimentally that methyl bisalkyl carbamates were self-crosslinked at high temperature due to the reactions of terminal methoxycarbonyl groups with secondary amide groups. In order to solve this problem, a new “hard segment-first” route was developed to prepare linear PUs, and the obtained PUs exhibited quite good mechanical properties but poor flexibility.²¹ In 2002, Rokicki and Piotrowska reported a new method for the synthesis of aliphatic PUs using ethylene carbonate, diamines and diols catalyzed by a tin coordination catalyst. The authors used 1,4-butanediamine and 1,6-hexanediamine to open the ring of ethylene carbonate to obtain bis(hydroxyalkyl)carbamate, which was then condensed with diols to obtain PUs while removing small molecule ethylene glycol.²⁴

The non-isocyanate routes are significant for the greening of the PUs industry, but the reported non-isocyanate routes of PUs synthesis still face some problems and challenges, such as difficulty in synthesizing PUs of high molecular weights, insufficient mechanical properties, long reaction time and by-product generation.^{12,25–29} In the PUs industry, polyester polyurethanes and polyether polyurethanes have their own advantages and disadvantages. Polyester polyurethanes have poor hydrolysis resistance, while polyether polyurethanes have poor mechanical and heat resistance properties. Polycarbonate polyurethanes overcome the disadvantages of both and have good weather resistance, bacteria resistance, hydrolysis resistance and excellent mechanical properties, and its good biocompatibility can also be used for biological materials.^{30–32}

In this work, we obtained high molecular weight and high performance TPCUEs using a non-isocyanate route of melt polycondensation and overcame some problems of non-isocyanate routes, making the approach very competitive in replacing isocyanate routes.

Experimental

Materials

DMC was obtained from Chengdu Kelong Chemicals Co., Ltd. 1,6-hexanediol (HDO), 1,6-hexanediamine (HDA), ethylene carbonate (EC) and dibutyltin oxide (DBTO) were purchased from Shanghai Macklin Biochemical Co., Ltd.

Synthesis of BHCH

Ethylene carbonate and 1,6-hexanediamine were added to a three-necked flask in a molar ratio of 2.2 : 1, and the reactions were maintained under nitrogen atmosphere and refluxed at 100 °C for 5 h. The products were recrystallized with distilled

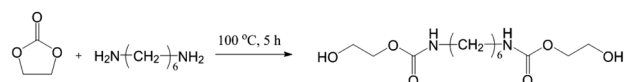


Fig. 1 Synthesis of BHCH.

water and the yields were about 89%. The ¹H NMR spectra of BHCH is shown in ESI (Fig. S1†). Fig. 1 shows the synthesis route of BHCH.

¹H NMR data (600 MHz, CDCl₃): δ (ppm) = 4.98 (NH); 4.25 (CH₂O); 3.89 (CH₂OH); 3.27 (CH₂NH); 2.75 (OH); 1.57 (CH₂-CH₂NH); 1.39 (CH₂CH₂CH₂NH).

Synthesis of PCDLs

PCDLs were prepared by a two-step method of ester exchange and polycondensation. DMC and HDO were added to a three-necked flask in a certain molar ratio, and the catalyst CH₃-COONa was added. The reaction was carried out at 125 °C for 4 h under atmospheric pressure, and then the reaction was heated to 150 °C for 5 h under 5 kPa. The obtained PCDLs were named as PCDL1000, PCDL2000, PCDL3000 (PCDL1000, PCDL2000, PCDL3000 indicated that the obtained PCDLs with molecular weights of 1000, 2000 and 3000, respectively). The ¹H NMR spectra of PCDL2000 is shown in ESI (Fig. S2†). Fig. 2 shows the synthesis route of PCDLs.

¹H NMR data (600 MHz, CDCl₃): δ (ppm) = 4.17 (CH₂O); 3.68 (OH); 1.74 (CH₂CH₂O, CH₂CH₂OH); 1.63 (CH₂OH); 1.48 (CH₂-CH₂CH₂O, CH₂CH₂CH₂OH).

Synthesis of TPCUEs

BHCH, PCDLs and catalysts were added to a three-necked flask, and a nitrogen atmosphere was maintained for the pre-polymerization reaction at a lower vacuum degree, followed by polycondensation at a higher vacuum degree. The products were quickly removed at the end of the reaction in the molten state. The products were named TPCUE_{m/n}, where *m* was the molecular weights of PCDLs and *n* was the hard segment content. For example, TPCUE1000/40 was the synthesized TPCUEs with a soft segment of PCDL1000 and a hard segment content of 40%. Fig. 3 shows the synthesis route of TPCUEs.

Characterization

The Mn, Mw and PDI of TPCUEs were determined by gel permeation chromatography (GPC) with waters 1525 & Agilent PL-GPC220, polystyrene as standard sample and DMF as solvent at a flow rate of 1 mL min⁻¹.

The FT-IR spectra was measured by the Thermo Fisher Nicolet 670 within the wavelength range of 4000 to 500 cm⁻¹ and the resolution was 4 cm⁻¹. The ¹H NMR spectra was measured by Bruker Avance NEO 600MHz spectrometer at 25 °C and the CDCl₃ was used as solvent.

The surface morphology of TPCUEs was observed by atomic force microscope (AFM, Bruker Dimension Icon) at room temperature, and the tapping mode was selected.

The X-ray diffraction (XRD) of TPCUEs were analyzed by a Rigaku Smart Lab diffractometer with a range of 5–90°.

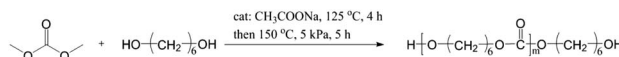


Fig. 2 Synthesis of PCDLs.



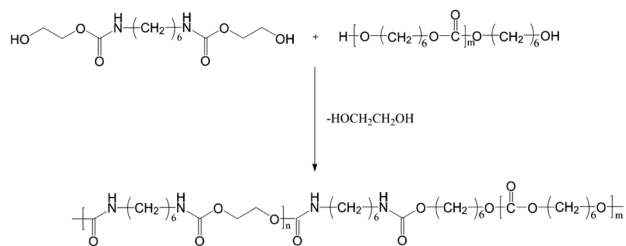


Fig. 3 Synthesis of TPCUEs.

The melting and crystallization behaviors of TPCUEs were measured on the TA DSC2500 analyzer under N_2 atmosphere, the samples were warmed up to 180 °C from 30 °C, then cooled down to -60 °C, and then warmed up to 180 °C for the second time with a temperature rise and fall rate of 10 °C min⁻¹.

The thermal stabilities of TPCUEs were performed by the TGA5500 thermogravimetric analyzer, the samples were heated under N_2 atmosphere with a temperature rise rate of 10 °C min⁻¹ and a temperature range of 30–600 °C.

The tensile testing was measured by a universal tensile tester (NKK 3010D), and the samples were made into standard dumbbell-type specimens based on the standard of ISO 527-2:1993. The tensile testing was tested at 25 °C and the stretching rate is 20 mm min⁻¹. When the samples were stretched to an elongation of 200%, the external force was removed, then the samples were left for 3 min and the effective length was measured. The Resilience (R_e) was calculated by the following equation:

$$R_e = \frac{2L_0 - (L - L_0)}{2L_0} \times 100\% \quad (1)$$

where L_0 is the original effective length of the samples, L is the effective length of the samples after stretching.

Results and discussion

Preparation of TPCUEs

A series of TPCUEs were synthesized with the optimized process conditions: DBTO catalyst dosage of 0.2 wt%, prepolymerization temperature of 120 °C, prepolymerization time of 1 h, polycondensation temperature of 180 °C, and polycondensation time of 1 h. The synthesized TPCUEs and the GPC data are shown in Table 1. Because the difference in the contents of the hard segment as well as the structures and molecular weights of the soft segment, the molecular weights of synthesized TPCUEs also varied. The M_n of synthesized TPCUEs were in the range of $3.0\text{--}7.6 \times 10^4 \text{ g mol}^{-1}$, and the M_w of synthesized TPCUEs were in the range of $4.1\text{--}19.3 \times 10^4 \text{ g mol}^{-1}$. The trend of molecular weights of TPCUEs was that the larger the hard segment contents and the soft segment molecular weights led to the larger molecular weights of TPCUEs.

Structures characterization of TPCUEs

Since the synthesized TPCUEs contain the same functional groups, a certain sample (TPCUE2000/50) was taken for FT-IR

Table 1 The GPC data of synthesized TPCUEs

| TPCUEs ^a | SS ^b | HS% ^c | M_n (g mol ⁻¹) | M_w (g mol ⁻¹) | PDI |
|---------------------|-----------------|------------------|------------------------------|------------------------------|------|
| TPCUE1000/40 | PCDL1000 | 40 | 30460 | 41160 | 1.35 |
| TPCUE1000/50 | PCDL1000 | 50 | 42590 | 66320 | 1.56 |
| TPCUE1000/60 | PCDL1000 | 60 | 39270 | 48430 | 1.23 |
| TPCUE2000/40 | PCDL2000 | 40 | 44000 | 67710 | 1.54 |
| TPCUE2000/50 | PCDL2000 | 50 | 50330 | 69520 | 1.38 |
| TPCUE2000/60 | PCDL2000 | 60 | 62040 | 147100 | 2.37 |
| TPCUE3000/40 | PCDL3000 | 40 | 48520 | 63160 | 1.28 |
| TPCUE3000/50 | PCDL3000 | 50 | 76740 | 193100 | 2.52 |

^a Reaction conditions: 0.2 wt% DBTO; 120 °C, 3 kPa, 1 h; then 180 °C, 300 Pa, 1 h. ^b SS: types of soft segments. ^c HS%: mass percentage of

the hard segments, $HS\% = \frac{m_1 - \frac{m_1}{M_1} \times M_e}{m_1 - \frac{m_1}{M_1} \times M_e + m_2} \times 100\%$, where m_1

and M_1 are the mass and molecular weight of BHCH, respectively; and M_e is the molecular weight of ethylene glycol, m_2 is the mass of PCDL.

characterization. The FT-IR spectra of the TPCUE2000/50 is shown in Fig. 4. As shown in Fig. 4, the sample had N–H stretching vibration peak at 3323 cm⁻¹, methylene stretching vibration peak at 2936 cm⁻¹ and 2864 cm⁻¹, free C=O absorption peak and hydrogenated C=O absorption peak in the carbamate bond at 1736 cm⁻¹ and 1685 cm⁻¹. 1530 cm⁻¹ and 1245 cm⁻¹ peaks were the C–N stretching vibration peak and C–O stretching vibration peak in the carbamate bond, respectively. 979 cm⁻¹ peak was C–O–C vibration peak in the carbonate group. The result of FT-IR spectra was in accordance with the structural features of TPCUE2000/50.

To further confirm the chemical structures of the TPCUE2000/50, the sample was analyzed by ¹H NMR (Fig. 5). In the ¹H NMR spectra of the sample, d ($\delta = 4.0$ ppm), e ($\delta = 3.2$ ppm), f ($\delta = 1.7$ ppm) and i ($\delta = 1.3$ ppm) were the proton characteristic peaks of the methylene on the hexamethylene chain segments, a ($\delta = 4.8$ ppm) was the proton characteristic peak of the carbamate bond, c ($\delta = 4.1$ ppm), g ($\delta = 1.5$ ppm) and h ($\delta = 1.4$ ppm) were the proton characteristic peaks of the methylene groups on the PCDLs chain segments, and b ($\delta = 4.2$ ppm) was the terminal hydroxyl peak of the PCDLs chain

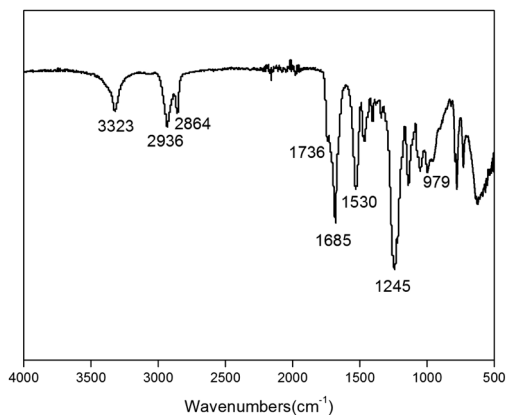


Fig. 4 FT-IR spectra of the TPCUE2000/50.



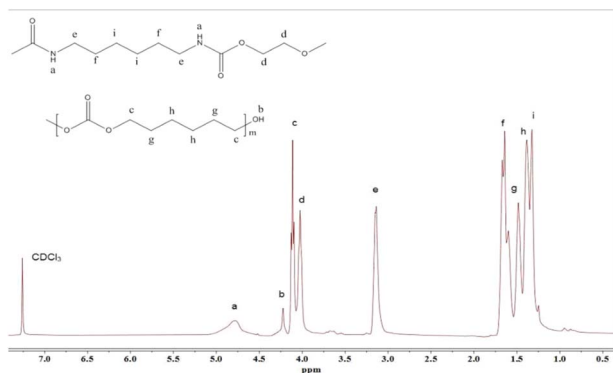


Fig. 5 ^1H NMR spectra of the TPCUE2000/50.

segments. The ^1H NMR spectra was consistent with the structural features of TPCUE2000/50, which further confirmed the chemical structures of the TPCUE2000/50.

Crystallization properties of TPCUEs

The crystallization properties of synthesized TPCUEs were analyzed by using XRD testing (Fig. 6). The crystallinity (X_c) of TPCUEs is listed in Table 2. As shown in Fig. 6, the intensity of two sharp diffraction peaks of the TPCUEs at 2θ of 21° and 23.5° , respectively, decreased with the increase of the hard segment contents, and finally formed a wide diffraction peak at 2θ of 19.6° . The appearance of diffraction peaks at 21° and 23.5° were typical diffraction peaks of PCDLs, which indicated that soft segment crystallization was the main source of crystallization of TPCUEs with lower hard segment contents. Due to the addition of hard segments, the regular structures of soft segments were destroyed. At the same time, there was a certain compatibility between soft segments and hard segments, and with the increase of hard segment contents, the hard segments dissolved in soft segments also increased, which decreased the degree of microphase separation and led to the decrease of crystallinity. Microphase separation arises because of the thermodynamic incompatibility of hard segments and soft segments, often combined with crystallization of either or both segments, drives their microphase separation into hard and soft

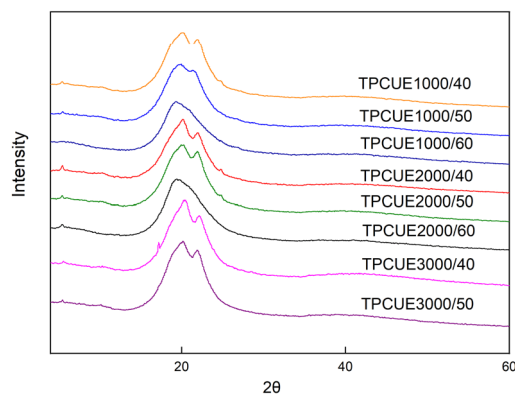


Fig. 6 The XRD diagrams of synthesized TPCUEs.

Table 2 The thermal properties data and crystallinity of synthesized TPCUEs

| TPCUEs | T_g ($^\circ\text{C}$) | T_m ($^\circ\text{C}$) | $T_{d,5\%}$ ($^\circ\text{C}$) | X_c (%) |
|--------------|----------------------------|----------------------------|----------------------------------|-----------|
| TPCUE1000/40 | -15.5 | 93 | 251 | 36 |
| TPCUE1000/50 | -7.9 | 112 | 246 | 19 |
| TPCUE1000/60 | -1.1 | 119 | 243 | 5 |
| TPCUE2000/40 | -17.2 | 103 | 265 | 39 |
| TPCUE2000/50 | -9.4 | 117 | 259 | 27 |
| TPCUE2000/60 | -1.5 | 122 | 245 | 9 |
| TPCUE3000/40 | -18.3 | 110 | 282 | 43 |
| TPCUE3000/50 | -10.7 | 117 | 262 | 33 |

phases.³³ The bright and dark areas of the AFM images confirmed the microphase separation of TPCUEs (Fig. 7). The peaks at 19.6° were diffraction peaks of hard segments, the wide and weak diffraction peak indicated weak crystallization. When the hard segment contents of TPCUEs reached 60%, the main crystallization came from the hard segments. In the case of the same hard segment contents, the larger the molecular weights of the PCDLs, the stronger the crystallization ability. This was because the longer soft segment chains were conducive to the microphase separation of TPCUEs.

Thermal properties of TPCUEs

The thermal properties of synthesized TPCUEs were measured by DSC testing (Fig. 8) and TGA testing (Fig. 9). The thermal properties data including glass transition temperature (T_g), melting temperature (T_m), and 5% mass decomposition temperature ($T_{d,5\%}$) are listed in Table 2.

As shown in Fig. 8, some samples showed exothermic peaks during the secondary heating process, which crystallized during heating, while others completed crystallization during cooling. The T_g of obtained TPCUEs ranged from -18 to -1°C , and the T_g moved toward higher temperature as the hard segment contents increased; the T_m ranged from 93 to 122°C , and the T_m increased with the increase of the hard segment contents. The increase in T_g with the increase in hard segment contents was due to the increase in the mixing of hard segments and soft segments, resulting in a decrease in the degree of microphase separation. The increase in T_m with the increase hard segment contents was due to the increase in the number of hydrogen

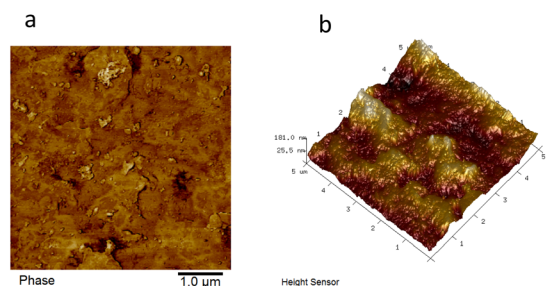


Fig. 7 AFM images of TPCUE2000/50 (a, phase image; b, 3D height image).



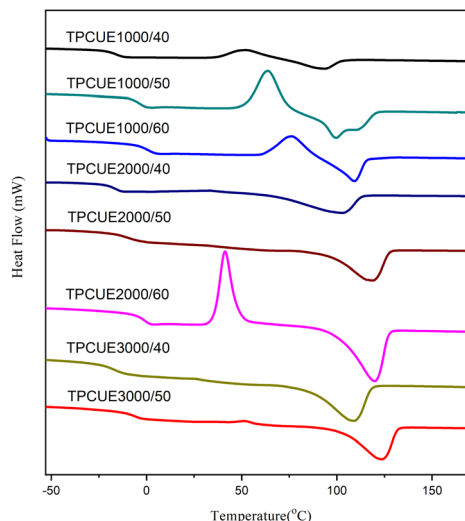


Fig. 8 The DSC curves of synthesized TPCUEs (secondary heating).

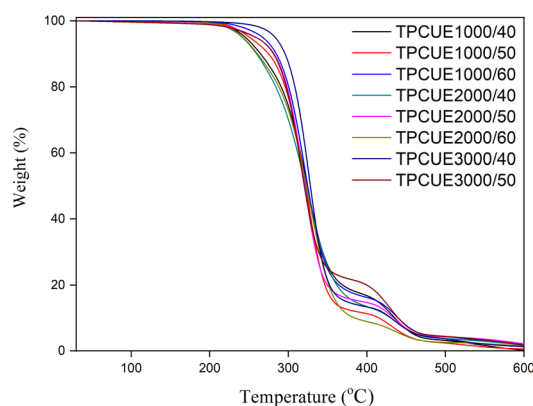


Fig. 9 The TGA curves of synthesized TPCUEs.

bonds with the increase in the proportion of hard segments, and the increase in the degree of physical cross-linking of the TPCUEs. At the same hard segment contents, the T_g of the TPCUEs declined as the molecular weights of the PCDLs increased, which correlated with the increase in degree of microphase separation of TPCUEs. And the T_m increased because of the increase of crystallinity.

As shown in Fig. 9, the thermal decomposition occurred on different temperature ranges and was divided into two stages. The two stages were attributed to the decomposition of different components. The first decomposition stage was the decomposition of the hard segments and partly soft segments, and the second stage was the decomposition of the soft segments only. Because the bond energy of the carbonate bond was higher than that of the carbamate bond, the hard segments were more easily decomposed than the soft segments. The thermal stability of the TPCUEs was good, and the $T_{d,5\%}$ were above 240 °C. The $T_{d,5\%}$ of TPCUEs decreased as the contents of hard segment increased, because the heat resistance of hard segments was weaker than that of soft

segments, and the decomposition of carbamate bonds became more obvious when the number of hard segments increased.³⁴ Moreover, the thermal stability of TPCUEs increased with the molecular weights of the PCDLs increased. As the molecular weights of PCDLs increased, the degree of microphase separation increased, resulting in a higher degree of physical cross-linking of the hard segment domains, thus increasing the initial degradation temperature.

Mechanical properties of TPCUEs

The stress–strain curves of synthesized TPCUEs are shown in Fig. 10, and the tensile data of the TPCUEs are listed in Table 3. All obtained TPCUEs exhibited good tensile strength, elongation at break and resilience. From the Fig. 10, it can be seen that the stress–strain curves of TPCUEs had the typical characteristics of elastomeric materials. From the data in Table 3, it can be seen that with the increase of the hard segment contents, the tensile strength and Young's modulus of the TPCUEs increased, but the elongation at break and resilience showed a gradual decrease. The rigid hard segments provided excellent mechanical strength to the TPCUEs through the formation of hydrogen bonds, while the hard segments aggregated to form the hard segment phase region and acted as physical cross-linking points in the soft segment phase, increasing the mechanical strength of the TPCUEs. While the physical cross-linking increased, which restricted the movement of the molecular chains and led to a decrease in elasticity. It was also clear from the data in Table 3 that the tensile strength, Young's modulus and elongation at break increased as the molecular weights of the PCDLs increased. This was due to the increase in the molecular weights of PCDLs, which led to an increase in the crystallinity of the soft segment domains thus showing higher tensile strength, while longer PCDLs chains increased the elongation at break. The obtained TPCUEs exhibited comparable or even better mechanical properties than isocyanate TPUEs (the Bayer's polycarbonate series TPU products, e.g., Desmopan 786 E and Desmopan 786 S, have a tensile strength of 35–40 Mpa, Young's modulus of 20–35 Mpa and an elongation at break of 500–600%).

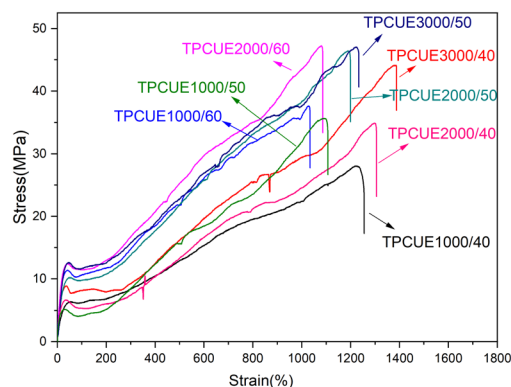


Fig. 10 The stress–strain curves of synthesized TPCUEs.



Table 3 The mechanical properties data of synthesized TPCUEs

| TPCUEs | Tensile strength (MPa) | Young's modulus (MPa) | Strain at break (%) | Resilience at 200% fixed-length (%) |
|--------------|------------------------|-----------------------|---------------------|-------------------------------------|
| TPCUE1000/40 | 28.1 | 13.8 | 1254 | 84 |
| TPCUE1000/50 | 35.7 | 20.7 | 1106 | 78 |
| TPCUE1000/60 | 37.6 | 31.0 | 1033 | 75 |
| TPCUE2000/40 | 34.9 | 18.7 | 1305 | 85 |
| TPCUE2000/50 | 46.3 | 22.2 | 1200 | 82 |
| TPCUE2000/60 | 47.3 | 32.7 | 1085 | 80 |
| TPCUE3000/40 | 44.1 | 22.4 | 1387 | 87 |
| TPCUE3000/50 | 47.0 | 24.1 | 1233 | 82 |

Conclusions

In this work, a series of TPCUEs with linear structures and high molecular weights were synthesized through a non-isocyanate route, and these TPCUEs exhibited good thermal properties and excellent mechanical properties, suitable for application in high performance elastomeric materials. The hard segment contents and soft segment molecular weights had a great influence on the properties of TPCUEs. With the increase of hard segment contents, the crystallization ability of TPCUEs weakened, T_g and T_m increased, thermal stability decreased, tensile strength increased and elongation at break decreased; with the increase of soft segment molecular weights, the crystallization ability of TPCUEs increased, T_g decreased, T_m increased, thermal stability increased, tensile strength and elongation at break increased.

This work does not use isocyanates, no solvent is needed, the reaction time is short and the by-product ethylene glycol generated can be recycled for the synthesis of ethylene carbonate, which is green and environmentally friendly. The TPCUEs prepared have no phenyl groups in its structures, so it does not yellow during use. In addition, the TPCUEs are soluble in organic solvents such as DMF, and have excellent strength and toughness, offering great prospects for industrialization.

Conflicts of interest

There are no conflicts to declare.

Acknowledgements

This work was supported by Sichuan Science and Technology Program (2020YFG0159).

Notes and references

- A. Cornille, R. Auvergne, O. Figovsky, B. Boutevin and S. Caillol, *Eur. Polym. J.*, 2017, **87**, 535–552.
- E. Delebecq, J. P. Pascault, B. Boutevin and F. Ganachaud, *Chem. Rev.*, 2013, **113**, 80–118.
- H. W. Engels, H. G. Pirkl, R. Albers, R. W. Albach, J. Krause and A. Hoffmann, *Angew. Chem., Int. Ed.*, 2013, **52**, 9422–9441.
- Z. S. Petrović and J. Ferguson, *Prog. Polym. Sci.*, 1991, **16**, 695–836.
- P. Kasprzyk, E. Sadowska and J. Datta, *J. Polym. Environ.*, 2019, **27**, 2588–2599.
- M. M. Mazurek, P. G. Parzuchowski and G. Rokicki, *J. Appl. Polym. Sci.*, 2014, **131**, 39764.
- J. E. Lockey, C. A. Redlich, R. Streicher, A. Pfahles-Hutchens, P. J. Hakkinen, G. L. Ellison, P. Harber, M. Utell, J. Holland and A. Comai, *J. Occup. Environ. Med.*, 2015, **57**, 44–51.
- J. H. Clark, T. J. Farmer, I. D. V. Ingram, Y. Lie and M. North, *Eur. J. Org. Chem.*, 2018, **2018**, 4265–4271.
- J. John, M. Bhattacharya and R. B. Turner, *J. Appl. Polym. Sci.*, 2002, **86**, 3097–3107.
- J. Guan, Y. Song, Y. Lin, X. Yin, M. Zuo, Y. Zhao, X. Tao and Q. Zheng, *Ind. Eng. Chem. Res.*, 2011, **50**, 6517–6527.
- K. A. Houton, G. M. Burslem and A. J. Wilson, *Chem. Sci.*, 2015, **6**, 2382–2388.
- L. Maisonneuve, O. Lamarzelle, E. Rix, E. Grau and H. Cramail, *Chem. Rev.*, 2015, **115**, 12407–12439.
- G. Rokicki, P. G. Parzuchowski and M. Mazurek, *Polym. Adv. Technol.*, 2015, **26**, 707–761.
- Y. Ecochard and S. Caillol, *Eur. Polym. J.*, 2020, **137**, 109915.
- O. Lamarzelle, G. Hibert, S. Lecommandoux, E. Grau and H. Cramail, *Polym. Chem.*, 2017, **8**, 3438–3447.
- A. Cornille, S. Dworakowska, D. Bogdal, B. Boutevin and S. Caillol, *Eur. Polym. J.*, 2015, **66**, 129–138.
- A. Cornille, G. Michaud, F. Simon, S. Fouquay, R. Auvergne, B. Boutevin and S. Caillol, *Eur. Polym. J.*, 2016, **84**, 404–420.
- C. Duval, N. Kébir, A. Charvet, A. Martin and F. Burel, *J. Polym. Sci., Part A: Polym. Chem.*, 2015, **53**, 1351–1359.
- D. Pan and H. Tian, *J. Appl. Polym. Sci.*, 2015, **132**, 41377.
- N. Kebir, S. Nouigues, P. Moranne and F. Burel, *J. Appl. Polym. Sci.*, 2017, **134**, 44991.
- Z. Shen, J. Zhang, W. Zhu, L. Zheng, C. Li, Y. Xiao, J. Liu, S. Wu and B. Zhang, *Eur. Polym. J.*, 2018, **107**, 258–266.
- P. Boisauvert, N. Kébir, A. S. Schuller and F. Burel, *Polymer*, 2020, **206**, 122855.
- D. Wolosz, P. G. Parzuchowski and A. Swiderska, *Eur. Polym. J.*, 2021, **155**, 110574.
- G. Rokicki and A. Piotrowska, *Polymer*, 2002, **43**, 2927–2935.
- Z. Wu, W. Cai, R. Chen and J. Qu, *Prog. Org. Coat.*, 2018, **119**, 116–122.
- M. S. Kathalewar, P. B. Joshi, A. S. Sabnis and V. C. Malshe, *RSC Adv.*, 2013, **3**, 4110–4129.



Paper

- 27 Z. Chen, N. Hadjichristidis, X. Feng and Y. Gnanou, *Macromolecules*, 2017, **50**, 2320–2328.
- 28 B. Bizet, E. Grau, H. Cramail and J. M. Asua, *Eur. Polym. J.*, 2021, **146**, 110254.
- 29 H. Gholami and H. Yeganeh, *Eur. Polym. J.*, 2021, **142**, 110142.
- 30 V. Garcia-Pacios, M. Colera, Y. Iwata and J. M. Martin-Martinez, *Prog. Org. Coat.*, 2013, **76**, 1726–1729.
- 31 M. Serkis, R. Poreba and J. Hodan, *J. Appl. Polym. Sci.*, 2015, **132**, 42672.
- 32 S. Kim and S. Liu, *ACS Biomater. Sci. Eng.*, 2018, **4**, 1479–1490.
- 33 S. Velankar and S. L. Cooper, *Macromolecules*, 1998, **31**, 9181–9192.
- 34 V. Garcia-Pacios, J. A. Jofre-Reche, V. Costa, M. Colera and J. M. Martin-Martinez, *Prog. Org. Coat.*, 2013, **76**, 1484–1493.

